Bioautomation, 2006, 5, 68 – 77 ISSN 1312 – 451X

Adaptive Phase Aberration Correction in Multi-Element Synthetic Aperture Imaging Systems

Vera Behar

Institute for Parallel Processing - Bulgarian Academy of Sciences
25-A, Acad. G. Bonchev Str., Sofia 1113, Bulgaria
E-mail: behar@bas.bg

Received: July 28, 2006 **Accepted: November 12, 2006**

Published: December 8, 2006

Abstract: *The problem of phase aberration correction in Multi-element Synthetic Aperture Focusing (MSAF) imaging systems is considered in this paper. In the MSAF imaging, the phase distortions caused by tissue inhomogenities can be adaptively estimated and compensated in two successive stages of signal processing – partial beamforming (low-resolution image) and synthetic aperture formation (high-resolution image). In this paper, two methods that can be used for phase correction at the stage of high-resolution image formation are studied – a Full Common Spatial Frequency (FCSF) technique and a Partial Common Spatial Frequency (PCSF) technique. The two techniques are based on the estimate of the cross-correlation function between low-resolution images, which is used for evaluation of phase aberration errors when forming a final high-resolution image. The effectiveness of each technique for phase aberration correction is determined by the improvement factor, which is defined as difference in dynamic range between the corrected image and the distorted one.*

Keywords*: Ultrasound imaging, Synthetic aperture imaging, Phase aberration correction, Simulation analysis.*

Introduction

Synthetic aperture imaging systems are a very attractive alternative to conventional imaging systems with phased array (PA) providing dynamically focused B-mode images in both transmit and receive at a higher frame rate. All the methods for synthetic aperture formation can be divided into the following classes – *Synthetic Receive Aperture* (SRA) technique [8], *Synthetic Transmit Aperture* (STA) technique[9], *Synthetic Aperture Focusing* (SAF) technique [10], and *Multi-Element Synthetic Aperture Focusing* (MSAF) technique [1, 6]. The *Multi-element Synthetic Aperture Focusing* technique is the best alternative method that acquires high-quality images at a very high frame rate. In the MSAF imaging, at each time, several array elements transmit an ultrasound pulse simultaneously emulating a single virtual transmit element in order to create a spherical wave. In the receive mode, a group of elements receive the echo signals simultaneously. At the next transmission a transmit sub-aperture is moved by L elements, and the process of transmission and reception is repeated again. This is continued for all positions of transmit/receive sub-apertures. The RF data associated with a single sub-aperture pair "transmitter-receiver" are synthetically focused producing low-resolution images (*partial beamforming*). The final high-resolution MSAF image is formed as a sum of low-resolution images after compensation of time delays associated with each sub-aperture pair "transmitter-receiver".

In the MSAF systems, a constant acoustic velocity of 1540 m/s is usually assumed when forming a final high-resolution image. The actual acoustic velocity in tissue, however, varies from 1450 m/s in fat to 1665 m/s in collagen. As a result, the low-resolution images are improperly focused and as a consequence, the final high-resolution image is degraded. This effect is called as aberration of MSAF images.

Aberrations of ultrasound images can be classified as *phase aberrations* or *distributed aberrations* [3]. The *phase aberrations* can be simulated as a near field thin screen. In this model it is assumed that a thin aberration layer lies at the surface of a transducer (Fig. 1).

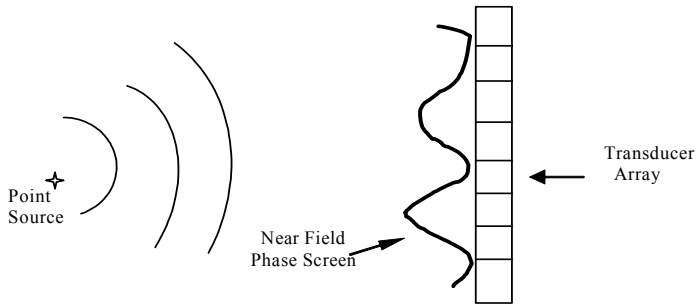

Fig. 1 Near – field thin phase screen

This is reflected in the fact that the signals received at different array elements are not aligned after beamforming, i.e. geometrical time delays compensation. To improve the image quality these time delays must be estimated and corrected. Various approaches can be used for phase correction – maximization of speckle brightness [7]; cross-correlation of echoes at adjacent elements [2]; minimization of the sum of absolute differences between samples at adjacent elements [5]; phase correction using speckle-look [4]. All these approaches are based on different methods for time delay estimation, which results in the accuracy of phase error estimates, stability and complexity of the algorithms. The *distributed aberrations* can be simulated as a cascade of mid-range phase screens. In this model it is assumed that the aberration layer lies away from the transducer [3]. This is reflected in distortions in the shape of the received pulses, which are not associated with time shifts.

In this paper are considered only aberrations that are associated with time shifts of low-resolution images (phase aberrations). Two methods for phase correction are studied here – a Full Common Spatial Frequency (FCSF) technique and a Partial Common Spatial Frequency (PCSF) technique, are described in [6]. In the MSAF system proposed in [6], only one element is dropped between transmit/receive sub-apertures, i. e. $L = 1$. Unlike [6], in the MSAF system presented here, the number of array elements between two neighbor transmit/receive sub-apertures is greater than unity, i.e. $L > 1$. The phase correction in this system is based on estimation of cross-correlation between neighbor low-resolution images in order to estimate phase errors between low-resolution images. The effectiveness of both techniques is evaluated by the improvement factor defined as difference in dynamic range between the corrected image and the distorted one.

MSAF imaging

Consider a MSAF system with the process of data acquisition shown in Fig. 2.

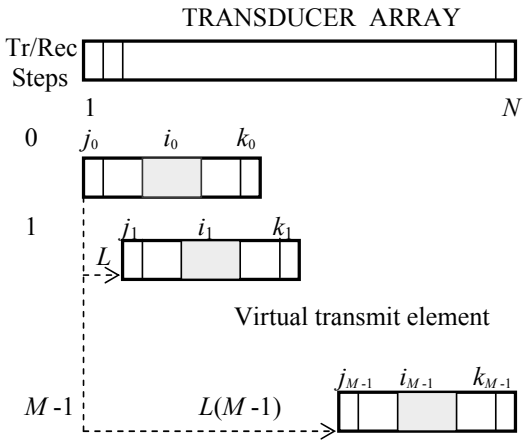

Fig. 2 Data acquisition in a MSAF imaging system

In each transmission, a group of N_t elements (transmit sub-aperture) is fired simultaneously to emulate a high power virtual transmit element located at the center of a transmit sub-aperture. The position of such a virtual transmit element within a virtual physical array is i_m (m = 0, …, M -1) [6]. A receive sub-aperture with N_r elements, located at a position i_m (m = 0, …, M -1) receives the echo RF signals. The process of transmission/reception is repeated for M different positions of a transmit/receive sub-aperture. Unlike [6], the number of array elements between two neighbor transmit/receive sub-apertures is grater than unity (L > 1), where $L = i_{m+1} - i_m$ for m = 0, …, M -1. In that case the number of transmissions needed to create a synthetic aperture equivalent to a virtual physical array with N elements is:

$$M = (N - N_r)/L + 1 \tag{1}$$

It is assumed that the signal processing is realized in the base band frequency domain, and (M×Nr) lines of complex amplitude are stored in the computer memory after quadrature detection. The process of image formation is carried out in two stages. Firstly, the complex amplitude of each low-resolution image associated with a single sub-aperture pair "transmitter-receiver" is obtained as a partial beamforming sum:

$$S_m(r,\theta) = \sum_{j=0}^{N_r-1} w_j U_{m,j}(t - \tau_{m,j}) \exp(i\Phi_{m,j}) \tag{2}$$

where $S_m(r,\theta)$ is the complex amplitude of the signal focused at a point (r, θ), $U_{m,j}$ is the complex amplitude of the echo signal received at the j^{th} element of the m^{th} receive sub-aperture, $\tau_{m,j}$ and $\Phi_{m,j}$ are the time delay and phase correction applied to the j^{th} element of the m^{th} receive

sub-aperture during beamforming, w_j is the weighting coefficient applied to the j^{th} element of a receive sub-aperture. The phases $\Phi_{m,j}$ used in the beamforming are evaluated as:

$$\Phi_{m,j} = 2\pi f_0 \tau_{m,j} \tag{3}$$

where f_0 is the central frequency of a transducer. The complex amplitude of the final high-resolution image is formed as a sum:

$$S_{MSAF}(r,\theta) = \sum_{m=0}^{M-1} S_m(r,\theta) \tag{4}$$

The final B-images are obtained from (4) after envelope detection, logarithmic compression, and then scan conversion.

Correlation between neighbor receive sub-apertures

The two-way time delays of the echo signals received at the j^{th} element of the m^{th} receive sub-aperture and at the k^{th} element of the $(m+1)^{th}$ receive sub-aperture are given by

$$\tau_{m,j} = (x_m + x_{m,j})\sin\theta / c \quad \text{and} \quad \tau_{m+1,k} = (x_{m+1} + x_{m,k})\sin\theta / c \tag{5}$$

where c is the velocity of sound (Fig. 3).

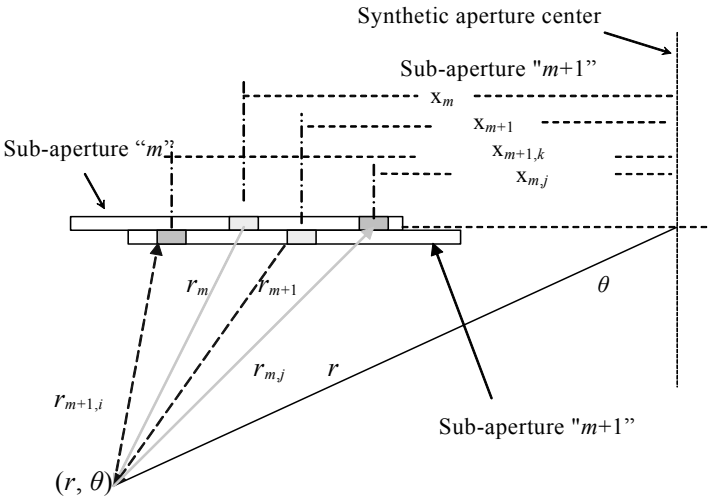

Fig. 3 The geometry of neighbor sub-apertures focusing

The location of receive sub-apertures (x_m , x_{m+1}) and the location of their elements ($x_{m,j}$, $x_{m+1,k}$) in reference to the synthetic aperture center are given by

$$x_m = (m - \frac{M-1}{2})\frac{\lambda}{2}L \quad \text{and} \quad x_{m+1} = x_m + \frac{\lambda}{2}L$$
$$x_{m,j} = x_m + (j - \frac{N_r - 1}{2})\frac{\lambda}{2} \quad x_{m+1,k} = x_{m+1} + (k - \frac{N_r - 1}{2})\frac{\lambda}{2} \tag{6}$$

where ($m = 1, ..., M$) and (k, $j = 1, ..., N_r$). It can be easy seen that elements k and j of the two neighboring receive sub-apertures have a common spatial frequency, if the time delay at element k is the same as at element j, i.e. $\tau_{m,j} = \tau_{m+1,k}$. In that case the indexes k and j satisfy the condition:

$$j = 2L + k, \tag{7}$$

where $j = 1, 2, ..., N_r$ and $k = 1, 2, ..., N_r$

According to (7), elements (2L+1), (2L+2), …, Nr of the m^{th} receive sub-aperture and elements 1, 2,…2L of the (m+1)th receive sub-aperture have common spatial frequencies. The number of common spatial frequencies is:

$$K_{SF} = \begin{cases} N_r - 2L, \text{ for } L = 0, 1, 2, ..., \dfrac{N_r - 1}{2} \\ 0, \quad \text{otherwise} \end{cases} \tag{8}$$

According to [5], the correlation coefficient between the echoes received at the two neighboring sub-apertures is evaluated as:

$$\rho_L = (N_r - 2L) / N_r, \quad L = 0, 1, ..., (N_r - 1) / 2 \tag{9}$$

Phase correction

Phase distortions caused by tissue motion or inhomogenities can be compensated at each of the two stages of MSAF signal processing – low-resolution image formation and high-resolution image formation. Phase estimation and phase correction across each receive sub-aperture is carried out at the stage of partial beamforming when forming low-resolution images. This operation can be made using the methods described in [2, 3, 4, 5, 7]. In this section we consider only the techniques for phase correction applied at the stage of synthetic aperture formation. Briefly, these techniques are used for compensation of phase errors between low-resolution images when a high-resolution image is formed. The concept of common spatial frequencies associated with neighboring receive sub-apertures can be successfully used for phase correction across a synthetic aperture [3, 4, 6, 7]. According to this concept the echo signals recorded from the neighboring receive sub-apertures are fully correlated over a limited kernel of sub-aperture elements. The cross-correlation function between neighboring low-resolution images is used for estimation of phase errors between low-resolution images. In this section we consider two techniques for adaptive phase correction described in [6].

For the m^{th} low-resolution image associated with the m^{th} receive sub-aperture, the corrections of time delay ($\tau_{cor,m}$) and phase ($\Psi_{cor,m}$) are evaluated as :

$$\tau_{cor,m} = \sum_{i=1}^{m} \Delta\tau_i \; ; \; \psi_{cor,m} = 2\pi f_0 \tau_{cor,m}, \; \Delta\tau_1 = 0 \tag{10}$$

The time delay difference ($\Delta\tau_i$) between the (i - 1)th low-resolution image and the i^{th} low-resolution image, used in (10), can be estimated using cross-correlation approach [6]:

$$\Delta\tau_i = p_i T_s,\ i = 2, \ldots, m \tag{11}$$

where p_i is the offset of the peak in a cross-correlation function and T_s is the sampling frequency. The cross-correlation function is evaluated as:

$$R_{i,i-1}(k) = \sum_{n=-Kt/2}^{Kt/2-1} s_i(nT_s)s_{i-1}((n+k)T_s) \tag{12}$$

According to [6], the reference signals S_i and S_{i-1} associated with the two neighboring receive sub-apertures can be calculated using the following techniques.

Full Common Spatial Frequency (FCSF) technique:

$$S_i(r,\theta) = \sum_{k=2L+1}^{N_r} w_k U_{i,k}(t-\tau_{i,k})\exp(j\Phi_{i,k})$$

$$S_{i-1}(r,\theta) = \sum_{k=1}^{N_r-2L} w_k U_{i-1,k}(t-\tau_{i-1,k})\exp(j\Phi_{i-1,k}) \tag{13}$$

Partial Common Spatial Frequency (PCSF) technique:

$$S_i(r,\theta) = \sum_{k=1}^{N_r} w_k U_{i,k}(t-\tau_{mi,k})\exp(j\Phi_{i,k})$$

$$S_{i-1}(r,\theta) = \sum_{k=1}^{N_r} w_k U_{i-1,k}(t-\tau_{i-1,k})\exp(j\Phi_{i-1,k}) \tag{14}$$

The corrected MSAF image is formed as:

$$S_{MSAF}^{cor}(r,\theta) = \sum_{m=1}^{M} S_m(t-\tau_{cor,m},\theta)\exp(j\psi_{cor,m}) \tag{15}$$

According to [6], the main steps of adaptive MSAF signal processing with phase error correction are shown in Fig. 4.

Simulation results

The effectiveness of each technique for phase correction can be estimated using the improvement factor C defined as difference in dynamic range of the corrected image and the distorted one:

$$C = D_{cor,dB} - D_{aber,dB} \tag{16}$$

where $D_{cor,dB}$ and $D_{aber,dB}$ are respectively the dynamic range of the corrected image and the distorted images. The improvement factor shows how well the image contrast is improved after phase correction.

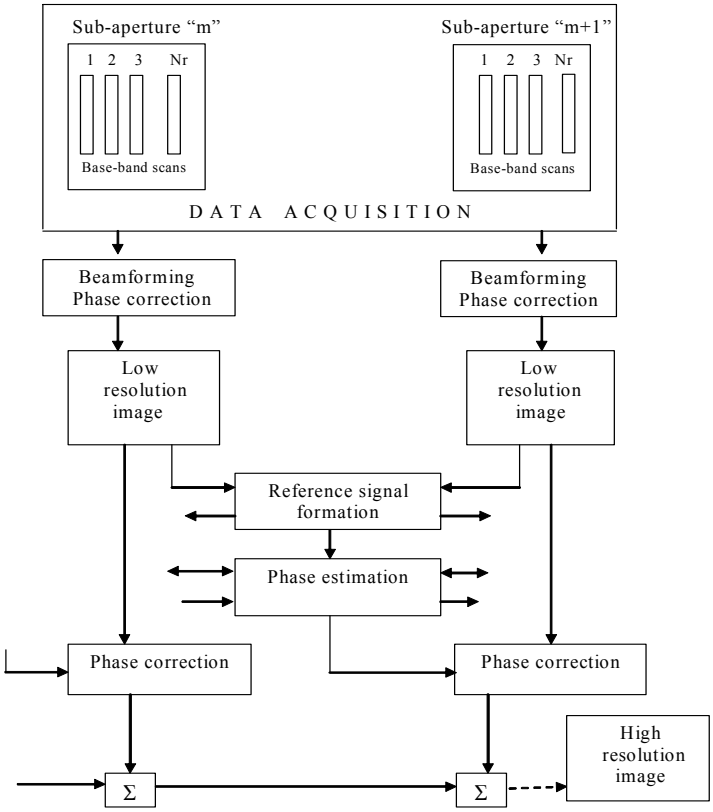

Fig. 4 Adaptive MSAF signal processing with phase error correction

In order to evaluate each technique for phase correction (FCSF and PCSF), two B-mode images (distorted and corrected) are simulated for:

- ($Nr = 15$, $M = 3$, $L = 1$) and ($Nr = 33$, $M = 5$, $L = 2$);
- SNR= 5 dB and 20 dB.

In simulations, it is assumed that a point target is located at a scan angle of 0˚ and at a distance of 70 mm. Both generated B-mode images, the distorted and the corrected, are displayed in dynamic range of –50 dB. The aberration time delays applied to each receive sub-aperture are simulated through random fluctuations of the velocity of sound. The velocity of sound is simulated as a Gaussian random variable distributed in range (1460, 1620) with mean of 1540. For simplicity, it is assumed that in the first receive sub-array the velocity of sound is 1540 m/s. For example, the graphical results for the case when the PCSF technique is applied are presented in Fig. 5 and Fig. 6. It is shown that after summation of five low-resolution images of a point target the final high-resolution image is unfocused due to the random fluctuations of the velocity of sound in each low-resolution image. As a result of phase correction, however, the final B-mode image is focused, and a single B-image is displayed. In result of phase correction, the image contrast is improved by 12 dB – for SNR = 5 dB and by 15 dB –for SNR = 20 dB.

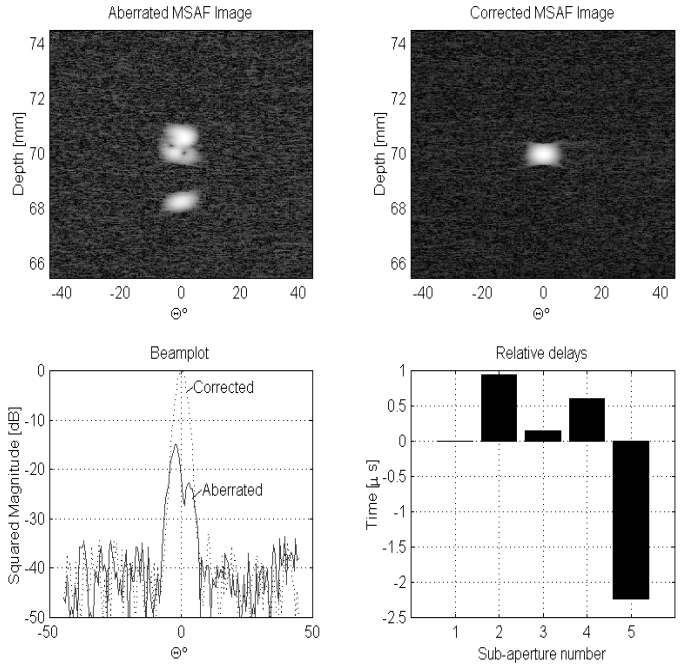

Fig. 5 B-images, beam pattern and aberration profile
(Nr = 33, M = 5, L = 2, SNR = 20 dB)

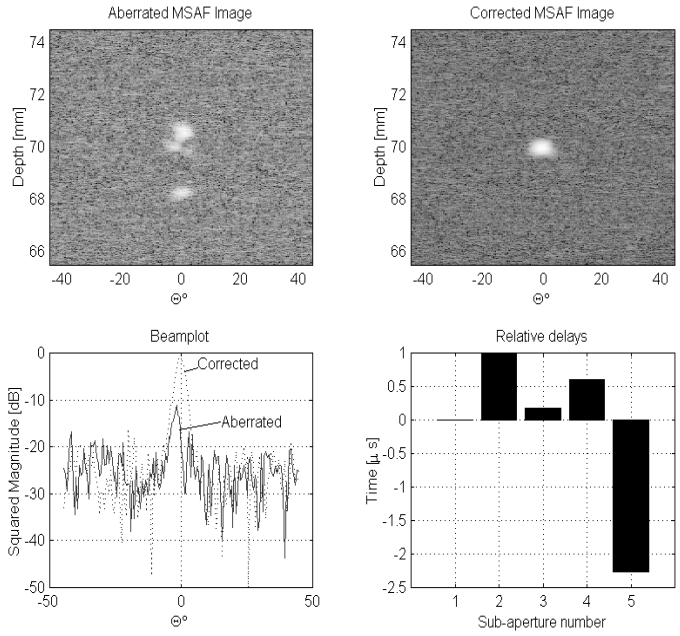

Fig. 6 B-images, beam pattern and aberration profile
(Nr = 33, M = 5, L = 2, SNR=5 dB)

The numerical results presented in Table 1 make possible to compare the effectiveness of each phase correction technique depending on the system parameters (*Nr*, *M*, *L*) and the SNR.

Table 1. Improvement factor

Nr	*M*	*L*	ρ	Improvement factor [dB]			
				SNR = 5 dB		SNR = 20 dB	
				Method			
				FCSF	PCSF	FCSF	PCSF
15	3	1	0.867	7	6.6	10	9.8
33	5	2	0.879	12	11.3	15	14.5

These results show that for the same system parameters, both techniques for phase correction are almost equivalent in effectiveness. As regards the system parameters, the second variant of a MSAF system, (*Nr* = 33, *M* = 5, *L* = 2), is more preferable providing higher values of the improvement factor.

Conclusions

The problem of phase aberration correction in MSAF imaging systems is considered. In the MSAF imaging, the phase distortions caused by tissue inhomogenities can be adaptively estimated and compensated at two successive stages of MSAF imaging – partial beamforming (low-resolution image formation) and synthetic aperture formation (high-resolution image formation). Two methods (FCSF and PCSF) that can be used for phase correction at the stage of high-resolution image formation are evaluated and estimated. The two techniques are based on estimation of the cross-correlation function between neighbor low-resolution images that is used to evaluate phase errors between these images. The effectiveness of each technique is determined by the improvement factor defined as difference in dynamic range between the corrected image and the distorted one.

Acknowledgment

This work is supported by the Center of Excellence BIS21++, Contract 016639, and the Bulgarian National Science Fund, Grant MI- 1506/05.

References

1. Cooley C., B. Robinson (1994). Synthetic Focus Imaging using Partial Data sets, Proceedings of 1994 Ultrasonics Symposium, 1539-1542.
2. Flax S., M. O'Donnell (1988). Phase Aberration Correction using Signals from Point Reflectors and Diffuse Scatterers: Basic Principles, IEEE Trans. on Ultrasonics, Ferroelectrics Frequency Control, 35, 758-767.
3. Gary C., P. Freiburger, W. Walker, G. Trahey (1997). A Speckle Target Adaptive Imaging Technique in the Presence of Distributed Aberrations, IEEE Trans. on Ultrasonics, Ferroelectrics Frequency Control, 44, 140-149.
4. Gary C., S. Worrell, P. D. Freiburger, G. E. Trahey (1994). A Comparative Evaluation of Several Algorithms for Phase Aberration Correction, IEEE Trans. on Ultrasonics, Ferroelectrics Frequency Control, 41, 631-642.

5. Karaman M., A. Atalar, H. Koymen, M. O'Donnell (1993). A Phase Aberration Correction Method for Ultrasound Imaging, IEEE Trans. on Ultrasonics, Ferroelectrics Frequency Control, 40, 275-282.
6. Karaman M., H. Bilge, M. O'Donnell (1998). Adaptive Multi-Element Synthetic Aperture Imaging with Motion and Phase Aberration Correction, IEEE Trans. on Ultrasonics, Ferroelectrics Frequency Control, 45(4), 1077-1087.
7. Nock L., G. Trahey (1989). Phase Aberration Correction in Medical Ultrasound using Speckle Brightness as a Quality Factor, Journal of Acoustics Society Am., 85, 1819-1833.
8. Nock L., G. Trahey (1992). Synthetic Receive Aperture Imaging with Phase Correction for Motion and for Tissue Inhomogeneities – Part I: Basic Principles, IEEE Trans. on Ultrasonics, Ferroelectrics Frequency Control, 39(4), 489-495.
9. Sverre H. et al. (1999). Method and Apparatus for Synthetic Transmit Aperture Imaging, USA Patent, Nº5951479, Sep. 14.
10. Ylitalo J., H. Ermert (1994). Ultrasound Synthetic Aperture Imaging: Monostatic Approach, IEEE Trans. on Ultrasonics, Ferroelectrics Frequency Control, 41(3), 333-339.